Micro and Nano Systems Letters

REVIEW

Open Access

Review on micro-gas chromatography system for analysis of multiple low-concentration volatile organic compounds: preconcentration, separation, detection, integration, and challenges

Yeongseok Lee[1], Hyeonwoo Son[1], Junwoo Lee[2] and Si-Hyung Lim[2*]

Abstract

As the dangers of volatile organic compounds (VOCs) and their potential as non-invasive diagnosis biomarkers have been reported, there has been a need for instrument capable of real-time and in-situ monitoring of multiple low-concentration VOCs in indoor air or human metabolites. A promising technology that can qualitatively and quantitatively analyze numerous VOCs as an alternative to conventional bench-top instruments is a micro-gas chromatography (μ-GC) system, which integrates three main components: a micro-gas preconcentrator, a μ-GC column, and a mini- or micro-detector fabricated using microelectromechanical system (MEMS) processes. This review covers the integration methods, features, and analysis capabilities of recently developed μ-GC systems and examines the materials, designs, and principles of the three main components. In addition, the challenging issues that must be addressed for the commercialization of this technology are discussed.

Keywords Volatile organic compounds, Indoor air, Biomarker, Micro-gas chromatography system, Micro-gas chromatography column, Micro-gas preconcentrator, Mini- or micro-detector

Introduction

Volatile organic compounds (VOCs) cause sick building syndrome or sick house syndrome, which includes a variety of respiratory illnesses and ailments, such as headaches, fatigue, and nausea [1, 2]. These VOCs are emitted from various materials integral to human indoor life, such as paints, wallpapers, adhesives, cosmetics, furniture, and petroleum-based products [3, 4]. Even at low concentrations, VOCs have several adverse effects over time, with greater effects on infants and people with pre-existing diseases [5, 6]. In particular, benzene and trichloroethylene were classified as Class 1 carcinogens by the International Agency for Research on Cancer [7]. Recently, the noninvasive diagnosis using VOCs in human metabolites has received considerable interest. In particular, exhaled breath has been examined as a metabolite secreted by the human body and was used to diagnose lung cancer with a high mortality rate. However, exhaled breath contains almost 1,000 types of low-concentration VOCs; thus, a high-performance instrument that can analyze VOCs in exhaled breath is required [8, 9]. The primary method used to detect low-level multi-species VOCs in the air and exhaled breath is thermal desorption–gas chromatography–mass spectrometry

*Correspondence:
Si-Hyung Lim
shlim@kookmin.ac.kr
[1] Department of Mechanical Systems, Kookmin University, Seoul 02707, Republic of Korea
[2] School of Mechanical Engineering, Kookmin University, Seoul 02707, Republic of Korea

(TD–GC–MS); however, this combined analytical instrument is large, expensive, time-consuming, and difficult to operate, making it inaccessible [10–12]. In addition, the complexity of sample preparation, sampling, transportation, and analysis demands manpower, cost, and time [13]. Most importantly, TD–GC–MS analyses cannot identify harmful VOCs and diagnose VOCs related diseases in real time on site. Thus, various studies on the development of μ-GC systems have been conducted over the past decade, which are miniaturized instruments capable of analyzing low-concentration, multispecies VOCs in the air and metabolites in real time and on-site [14–24]. μ-GC systems incorporate devices based on MEMS technology, with the key components being a micro-gas preconcentrator (μ-PC) used to increase analyte concentrations and overcome detection limits, a micro-gas chromatography(μ-GC) column to elute individual gases over time to provide selectivity, and a detector with various sensing mechanisms. Various studies have been conducted to develop and partially integrate these key components to detect specific VOCs. For example, the hybrid MEMS gas chromatograph, developed by the Zeller's group at the University of Michigan in 2005, is considered one of the pioneering μ-GC systems based on the above components and integration [25]. Since then, many systems capable of analyzing multispecies VOCs relevant to air quality have been developed, which vary in terms of detectable VOCs, detection time, detection limit, and sampling time depending on the material type, geometric design, analysis process, and device integration method.

Several review articles have been reported to effectively provide information about μ-GC systems [26–28]. While previous reviews on μ-GC systems have focused on detailed introductions and comparisons between the key components such as μ-GC, this review will directly compare recently developed μ-GC systems and describe how certain limitations have been overcome from a system perspective. In addition, this review examines how each of these key components has replaced TD–GC–MS to provide a better understanding of μ-GC systems. Therefore, the various features of recently reported μ-GC systems obtained using device integration/configuration methods are characterized, and the specific characteristics and analytical performance of the main components are reviewed in terms of material, design, and principle. Finally, challenging issues regarding popularization and commercialization are discussed.

Micro gas chromatography system

As shown in Fig. 1, the basic configuration and analysis process of the system are similar to those of the TD–GC–MS system used to analyze low-concentration multiple VOCs and can be considered a miniaturized version of TD–GC–MS [29, 30]. This review divides the existing large commercial TD–GC–MS system into three systems and describes how each component has been replaced in the μ-GC system.

First, TD comprises a TD tube and TD equipment, and this configuration is referred to as the TD system [29, 31]. The TD system improves the sensitivity of TD–GC–MS by converting low-concentration VOCs into high-concentration VOCs, and for this purpose, it operates in two steps: preconcentration and TD. In the preconcentration step, the TD tube is filled with adsorbent materials, such as activated carbon, zeolite, activated alumina, carbon nanotubes, and graphene, which easily adsorb gases owing to their porosity and high specific surface area and play a role in continuously adsorbing trace amounts of VOCs over a period via a pump and storing them in

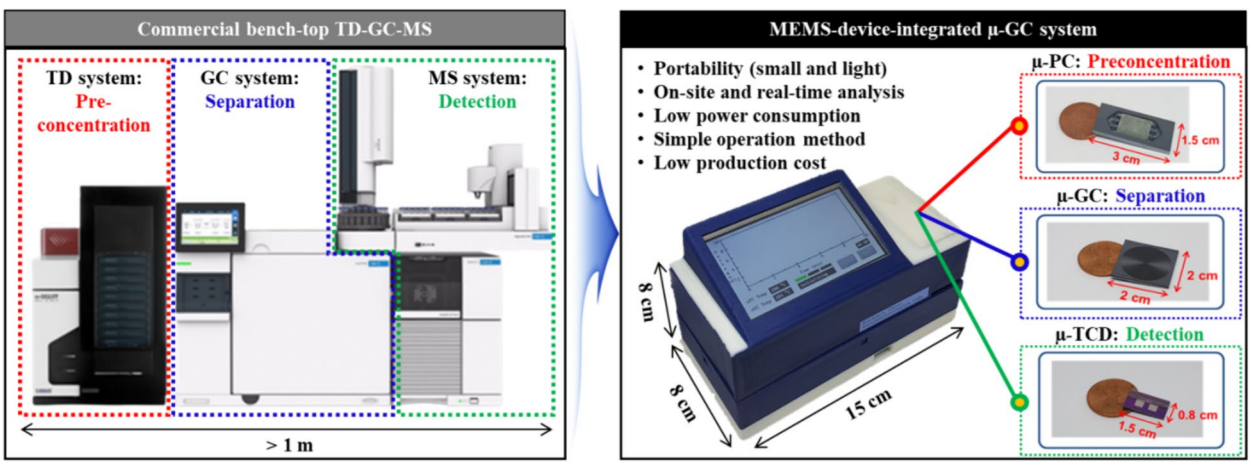

Fig. 1 Commercial bench-top TD–GC–MS system and MEMS-device-integrated μ-GC system

the TD tube. In the TD step, large amounts of VOCs adsorbed on the adsorbent in the TD tube are released upon rapid heating, and the concentrations of the thermally desorbed VOCs can be several orders of magnitude higher than the initial concentrations collected in the preconcentration step. The μ-PC, one of the key components in μ-GC systems, is fabricated via the MEMS process and is a chip developed to replace the entire configuration of a TD system on a centimeter scale (Fig. 2a) [29, 31, 32]. Inside the μ-PC chip, cavities with different structural features can pack and hold adsorbents. These cavities are connected with inlets and outlets that can import and export VOCs during the preconcentration and TD steps, respectively.

In addition, heater patterning is generally deposited on the backside of the chip, or the entire chip is coiled with metal wires to enable heating as TD equipment. The GC system of TD–GC–MS comprises a GC column packed or coated with a stationary phase to allow complex VOC mixtures to elute at different points over time and an oven to increase the resolution, selectivity, and repeatability of GC separations. Recently, capillary GC columns coated with a thin stationary phase, which mainly comprise polydimethylsiloxane (PDMS) and are easily modified using various functional groups, have been widely used owing to the disadvantages of packed-type columns with low separation efficiency owing to diffusion in the stationary phase, low plate number (representative performance index of the column), and high pressure. Figure 2b shows the μ-GC device that replaces the GC system, which comprises an oven and a packed/capillary GC column [33–36]. A capillary GC column is a thin, long fused silica tube with an inner diameter range of 0.1–0.53 mm and a length range of 15–60 m. Apart from the stationary phase, the length of the column has the greatest impact on separation performance. To achieve some of the lengths of a typical GC column in a centimeter-scale MEMS device, a deep reactive ion etching (DRIE) process is used. Using DRIE, a channel with a width of tens to hundreds of micrometers is elongated to achieve a channel length of 0.3–2 m at a chip scale of centimeters. The front side of the μ-GC device, which is dug out to form a channel, is mostly covered with glass and sealed using anodic bonding, allowing the fluid to flow in only one direction via the inlet and outlet. In addition, a heater patterning is deposited on the backside to replace the role of a GC oven. A resistive temperature detector (RTD) is often used in the μ-PC to check the temperature, but in μ-GC, an RTD is essential because temperature has a major impact on separation performance. Separation in GC is achieved by ensuring that a particular gas always has the same retention time (RT). The RT can be varied using temperature and the flow rate of the carrier gas, and by controlling these two factors, conditions for high resolution, selectivity, and efficiency can be established. The flow rate is a factor that cannot be controlled by GC; it is controlled using other parts in the system. By regulating the voltage applied to the heater based on the temperature measured using the RTD, constant conditions can be maintained to achieve high repeatability.

Although the MS detector linked to TD–GC can be replaced with a photoionization detector (PID) or flame ionization detector (FID), it is still considered a golden standard for analyzing low-concentration complex VOCs in air and human metabolites owing to its high sensitivity and ability to estimate unknown gases. Currently, micro-MS detectors with centimeter-scale components suffer from reduced resolution and sensitivity owing to limited ion separation space and are difficult to access because of their complex configuration comprising an ionization source, mass analyzer, and detector. Therefore, various detector devices such as the mini/micro-PID, micro-thermal conductivity detector (μ-TCD), capacitive detectors, metal oxide semiconductors, and chemiresistors are being used to replace the conventional large MS or FID detector (Fig. 2c) [30, 37–40]. Most of these detectors are fabricated using MEMS processes and have a centimeter scale for association with microfluidic devices, such as μ-PC and μ-GC.

By integrating the three main devices described above, a miniaturized μ-GC system was developed to replace the existing commercial TD–GC–MS system. Table 1 includes brief descriptions including the size, weight, key devices, and performance of the various systems reviewed in this study [15–24]. The details of the analysis process vary from system to system but can be summarized as shown in Fig. 3. The analysis process can be divided into three steps: a preconcentration step, a TD step, and a separation/detection step. First, in the preconcentration step, low-concentration VOCs are accumulated on a μ-PC at a certain flow rate for a specific period, and VOCs that are not adsorbed during the PC step are vented using a valve to prevent them from flowing into the μ-GC system or detector. Moreover, in the TD step, the VOCs converted to high concentrations are thermally desorbed using the heater patterned on the μ-PC. In the separation/detection step, thermally desorbed high-concentration VOCs are injected into the μ-GC system, and the heater and RTD are used to provide selectivity using either an isothermal mode that maintains a specific temperature or a programmed mode that ramps to higher temperatures at a constant ramping rate. VOCs eluted at different times from the end of the μ-GC system are detected as electrical signals using various detectors. This analysis process results in a two-dimensional graph

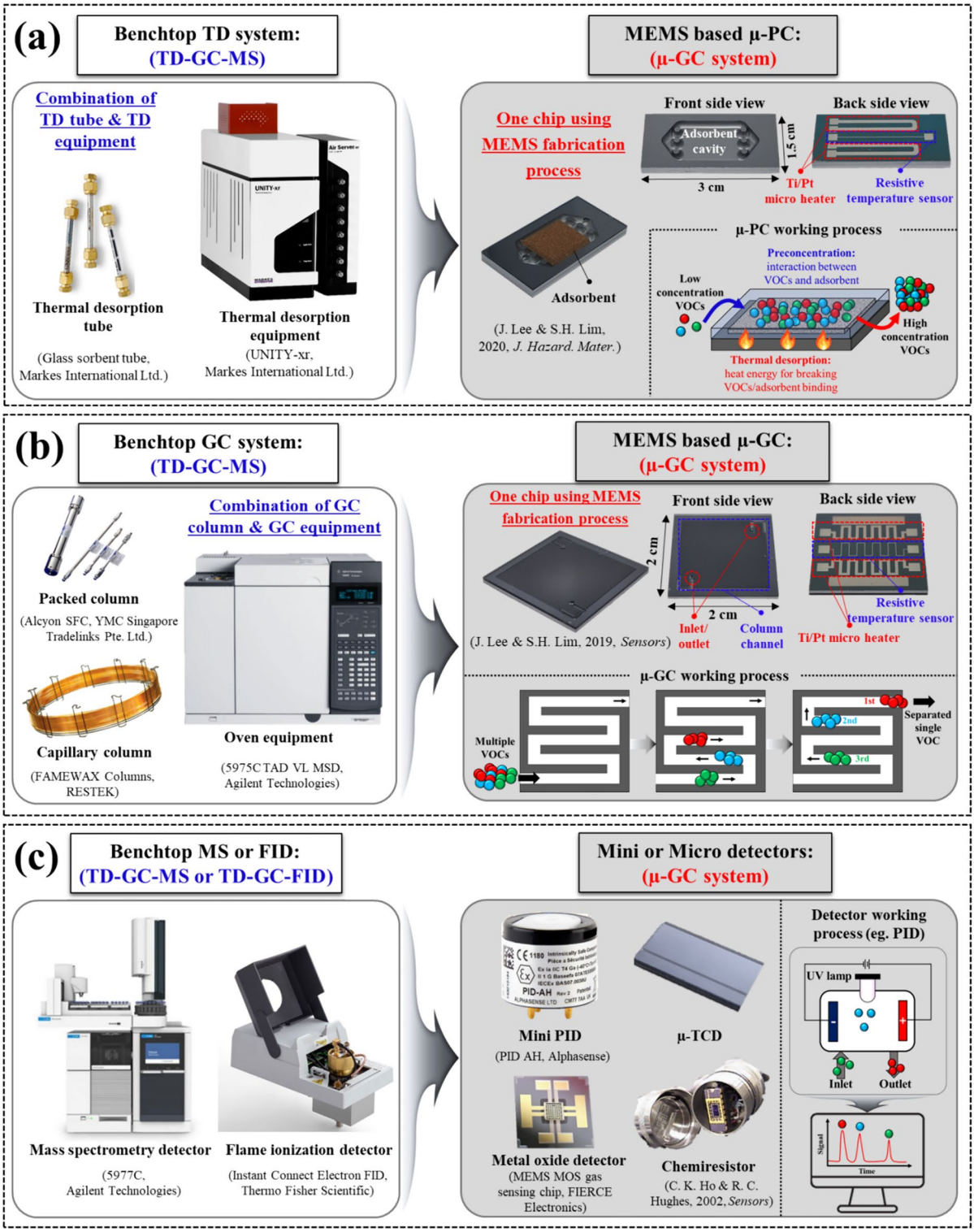

Fig. 2 Introduction to devices, equipment, and systems within TD–GC–MS and μ-GC systems. **a** TD system and μ-PC, **b** GC system and μ-GC, and **c** MS/FID and mini/micro-detectors [36] ©2002 MDPI. All rights reserved

Table 1 Recently developed μ-GC systems and their detailed configurations and performance

System name	Year	Size	Weight	Preconcentrator	GC column	Detector	LOD	Target VOCs	Analysis time
Zebra GC system [15]	2015	30 × 15 × 10 cm^3 (4.5 L)	1.8 kg	Microstructure type μ-PC	Serpentine μ-GC	μ-TCD	Sub 100 ppb	6 VOCs	1 min
iGC3.c2 system [16]	2016	Not described	Not described	U-shaped channel cantilever μ-PC	Serpentine μ-GC	Capacitive detector	10 ppb	19 VOCs	10 min
μGC system [17]	2016	16 × 11 × 11 cm^3 (1.94 L)	Not described	Microstructure type μ-PC	Serpentine circular μ-GC	Chemiresistor	15 ppb	7 VOCs	5 min
2-D GC × GC device [18]	2016	60 × 50 × 10 cm^3 (30 L)	5 kg	Cavity type μ-PC	Commercial capillary column	PID	Not described	50 VOCs	22 min
PEMM-1 [19]	2018	19 × 30 × 14 cm^3 (7.98 L)		Microstructure type μ-PC	Square spiral μ-GC	Chemiresistor array	100 ppb	24 VOCs	2.5 min
PEMM-2 [20]	2019	20 × 15 × 9 cm^3 (2.7 L)	2.1 kg	Microstructure type μ-PC	Square spiral μ-GC	Chemiresistor array	33 ppb	21 VOCs	3.5 min
Compact GC platform [21]	2019	12 × 8 × 7.5 cm^3 (0.72 L)	Not described	Not described	Square spiral μ-GC	μ-TCD or PID	1 ppb	7 VOCs	9 min
Compact prototype GC [22]	2019	32 × 29 × 14 cm^3 (12.99 L)	5 kg	Cavity type μ-PC	Commercial capillary column	PID	0.2 ppb	4 VOCs	16 min
Portable GC [23]	2020	35 × 26 × 15 cm^3 (13.65 L)	5 kg	Tube type PC	Commercial capillary column	PID	0.13 ppb	4 VOCs	10 min
μGC-PID [24]	2021	27 × 24 × 10 cm^3 (6.48 L)	Not described	Tube type PC	Square spiral μ-GC	μ-PID	0.18 pg	17 VOCs	10 min

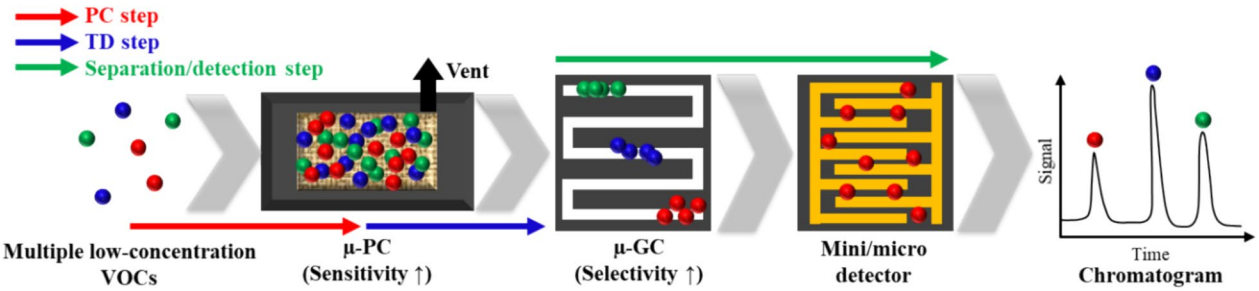

Fig. 3 Diagram of the analysis process for low-concentration VOCs using the μ-GC system

called a chromatogram with a time axis and an electrical signal axis, enabling qualitative and quantitative analysis of different VOCs.

The μ-GC systems reviewed in this work mostly follow the above analytical process and device integration (Fig. 4). Typically, Fig. 5a,b are considered to be schematic diagrams of a typical μ-GC system that includes each key components as well as other devices such as pump and valve. However, other systems different from the presented basic integration method or analysis process have also been developed by considering the newly developed device, targeted VOCs, system application, and miniaturization. First, the Zebra GC system used the μ-GC column and the μ-TCD as a single monolithic chip to prevent band broadening and fluidic interfaces that may result from integrating individual devices (Fig. 5c) [15]. Further, by uniting two devices as one, a spatial advantage was achieved. Reducing spatial constraints to a temperature gradient using a mesoporous polymer, and through this, the valve can be removed (Fig. 5d) [16]. This allowed for a large spatial advantage and simple analysis process configuration. The compact GC platform also utilized a silicon fluidic motherboard (FMB) connecting the μ-PC and the μ-GC system to free up space, ensure reliability against leaks, and prevent sample condensation at the low-temperature connection part (Fig. 5e) [21]. The silicon FMB comprises three silicon wafers and five membrane valves, and all interconnection parts are

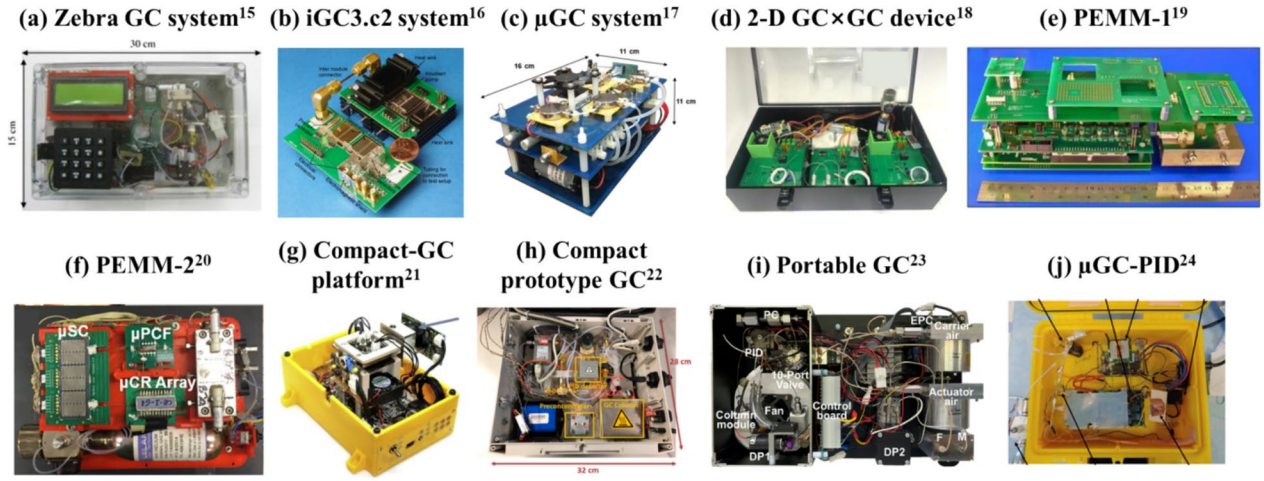

Fig. 4 Photographs of MEMS-device-integrated μ-GC systems. **a** Zebra GC system [15] ©2015 Elsevier. All rights reserved, **b** iGC3.c2 system [16] ©2016 Springer Nature. All rights reserved, **c** μGC system [17] ©2016 IEEE. All rights reserved, **d** 2-D GC×GC device [18] ©2016 American Chemical Society. All rights reserved, **e** PEMM-1 [19] ©2018 Springer Nature. All rights reserved, **f** PEMM-2 [20] ©2019 American Chemical Society. All rights reserved, **g** compact-GC platform [21] ©2020 Elsevier. All rights reserved, **h** compact prototype GC [22] ©2019 MDPI. All rights reserved, **i** Portable GC [23] ©2020 Elsevier. All rights reserved, and **j** μGC-PID [24] ©2021 American Chemical Society. All rights reserved

sealed using μ-O-rings. Owing to this structure, the compact GC platform has the smallest volume of any μ-GC system developed to date. These μ-GC systems achieve miniaturization while increasing performance, reliability, and repeatability.

In addition to the challenge of breaking through spatial constraints, some systems demonstrate more analytical performance-related configurations and integration methods. First, PEMM-1 and PEMM-2 used a pretrap device filled with the Carbopack series or coated with PDMS (Fig. 5f, g) [19, 20]. The pretrap device was installed in front of the μ-PC to remove interfering VOCs with low volatility for efficient monitoring of targeted VOCs. In contrast, a portable GC×GC device that uses two-dimensional (2D) GC to monitor all VOCs was developed (Fig. 5h) [18]. Because the stationary phase of most μ-GC systems utilizes a nonpolar stationary phase, the separation and detection of polar molecules are not easy, and the coelution of targeted nonpolar and polar VOCs cannot be avoided. However, the portable GC×GC device separates and detects nonpolar VOCs using the first one-dimensional (1D) nonpolar column and PID and transfers them to the 2D polar columns connected behind the 1D column by opening and closing the valve at specific times using a μ-Deans switch. Four additional 2D polar columns and their respective PIDs provide secondary detection of the VOC signal received from the switch. Afterward, using an algorithm that reconstructs all PID data, the portable GC×GC device detects 50 types of VOCs, the largest number among the systems developed to date.

Micro gas preconcentrator (μ-PC)

A miniaturized PC that replaces the TD system was first developed by Dave et al. in 1969, and initially, a tube type with the adsorbent packed in the tube and thermally desorbed by wrapping a hot wire was commonly used [41]. With the development of the first silicon wafer-based GC by Terry et al. in 1979, MEMS-process-based μ-PCs applicable to microfluidic systems began to be developed [42]. The μ-PC, which improves the sensitivity of the system using reversible gas adsorption and desorption phenomena, has been developed in various designs depending on the adsorbent and the microstructures formed inside [43–45]. Because the design of μ-PCs, including heating technology for the TD of VOCs, has various effects on adsorption performance, various studies have been conducted to develop the optimal design. These designs can be divided into cavity-, film-, and microstructure-type designs [46–48]. Further, the selection and development of the adsorbent is a large factor in determining the performance of the μ-PC (i.e., adsorption capacity and preconcentration factor). Representative adsorbent materials based on reversible physical adsorption/desorption can be divided into five types: polymer-, carbon-, oxide-, silicon-, and metal–organic framework (MOF)-type adsorbents [49–55]. In this chapter, the design and adsorbent materials, which are the biggest factors in determining the performance of the μ-PC, are examined in detail for each system and other developed μ-PC.

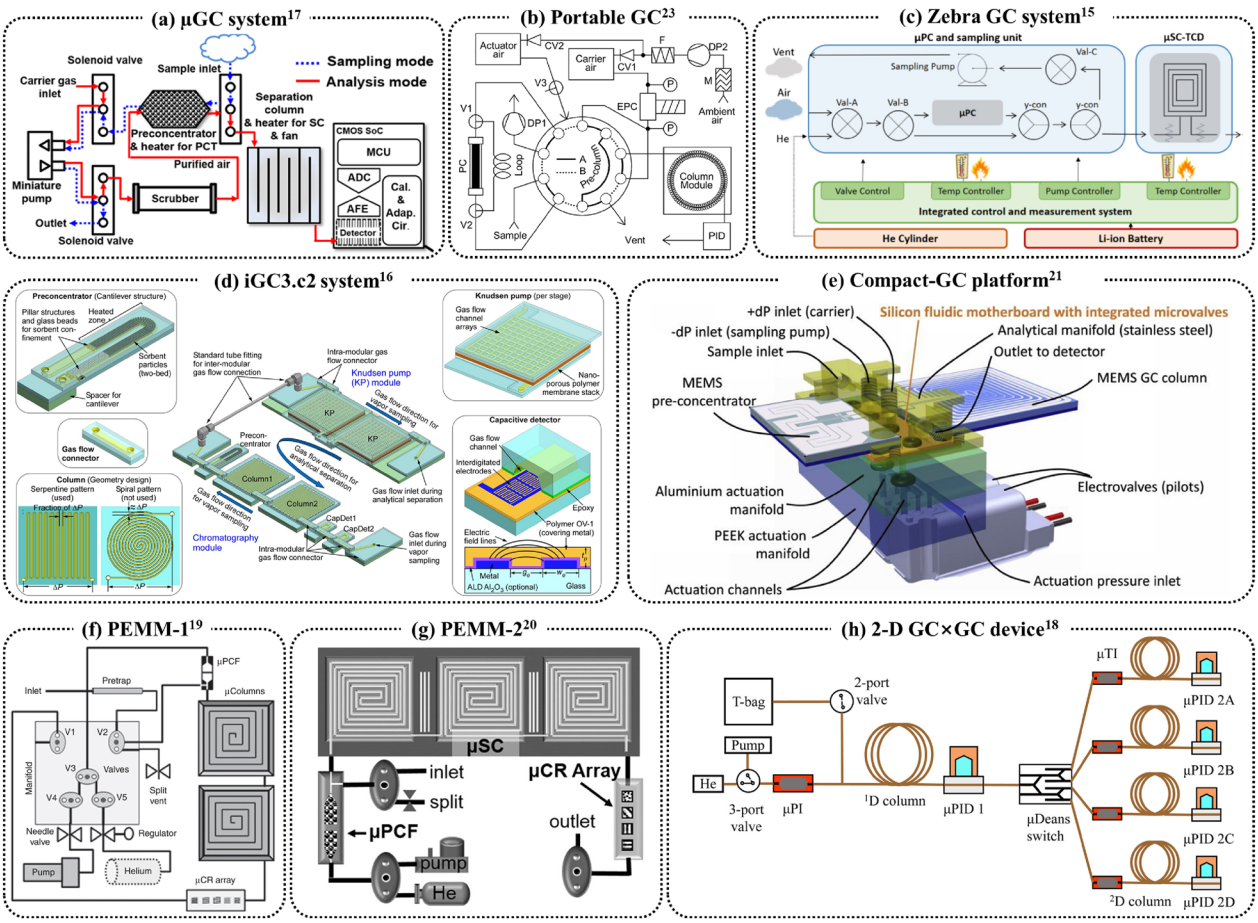

Fig. 5 Schematic diagrams of the μ-GC systems. **a** μGC system [17] ©2016 IEEE. All rights reserved, **b** Portable GC [23] ©2020 Elsevier. All rights reserved, **c** Zebra GC system [15] ©2015 Elsevier. All rights reserved, **d** iGC3.c2 system [16] ©2016 Springer Nature. All rights reserved, **e** compact-GC platform [21] ©2020 Elsevier. All rights reserved, **f** PEMM-1 [19] ©2018 Springer Nature. All rights reserved, **g** PEMM-2 [20] ©2019 American Chemical Society. All rights reserved, and **h** 2-D GC × GC device [18] ©2016 American Chemical Society. All rights reserved

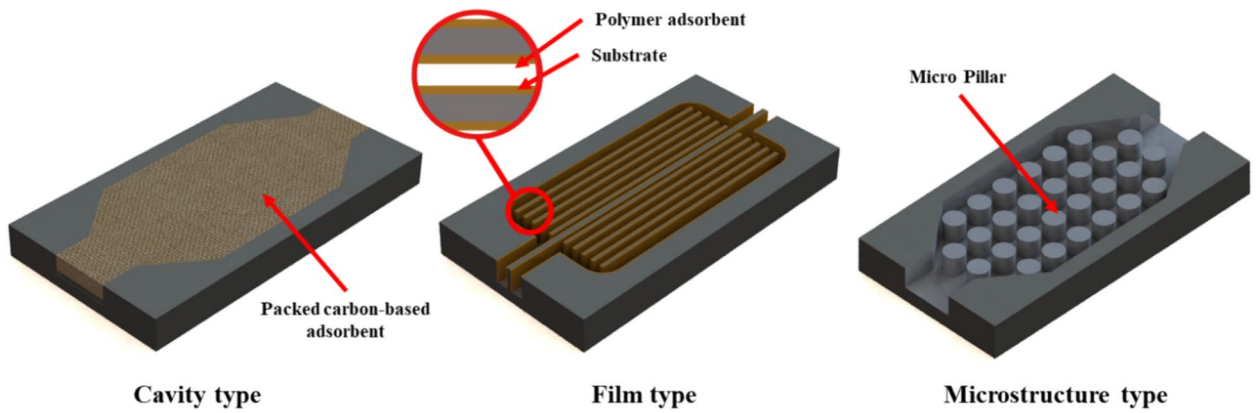

Fig. 6 Three main design types of the MEMS-based μ-PC

μ-PC design

Figure 6 shows the three main design types of the MEMS-based μ-PC. The first is the cavity-type design, where the adsorbent is packed in an empty space; the second is the film-type design, where the adsorbent is thinly coated on a channel or plane; the third is the microstructure-type design, where a structure is formed within the cavity and coated or packed with the adsorbent. The cavity- and film-type designs are determined by the adsorbent. Carbon-based adsorbents are mainly applied to the cavity type and have a large adsorption capacity owing to the high absolute mass of the adsorbent but are characterized by a high pressure drop. Polymer-based adsorbents are applied to the film-type design, which has a small adsorption capacity owing to the low mass of the adsorbent compared to that in the cavity-type design but offers a low pressure drop. Further, the microstructure-type design has been developed as a result of research conducted to increase the adsorption efficiency. As the μ-PC is applied to microfluidic systems, the inlet and outlet portions are exceedingly small, whereas the adsorbent packing area is wider and bulkier than the inlet and outlet portions. Because this structure does not allow the flow of VOCs beyond the line between the inlet and outlet sections, researchers have conducted studies to optimize the constant flow distribution across the adsorbent cross section. The compact prototype GC applied a manifold fluidic system to have a uniform flow velocity distribution, as shown in Fig. 7a [22]. In addition, the μGC system used a μ-PC to improve the flow velocity distribution by forming numerous vertical microneedle structures in the cavity while generating turbulence to increase the interaction between the adsorbent and VOCs (Fig. 7b) [17, 56]. An additional requirement for μ-PCs is to have a short peak bandwidth with low power consumption, necessitating in-depth manufacturing of the heater and considering heat transfer characteristics, uniform heat distribution, and thermal isolation in the design [57]. Figure 7c shows an example of a μ-PC with a cantilever structure that minimizes heat loss via thermal isolation in the iGC3.c2 system [16].

μ-PC adsorbent

The five main types of adsorbents have been developed in the order of polymer-, carbon-, oxide-, silicon-, and MOF-type adsorbents [58]. However, the types of sorbents currently in use are very limited and are mostly carbon-based adsorbents, such as Carbopack, Carbosieve, and the Carbograph series, as shown in Table 2. The Zebra GC system is the only μ-GC system reviewed in this paper that utilizes a polymer adsorbent, Tenax TA, coated on a microstructure formed in the cavity [15]. This μ-PC was found to increase the concentration up to 973 times, and in the system, it was preconcentrated for 2 min at a flow rate of 1 mL·min^{-1} and desorbed at 200 °C for 12 s [59]. The compact prototype GC utilized a μ-PC with a commercial MOF called Basolite C300 (HKUST-1) in combination with a heating cartridge desorption tool [22]. In addition, the portable GC utilized a conductive CNT sponge adsorbent developed as a PC by packing it in a glass tube [23]. Owing to its high thermal conductivity, the CNT sponge showed the shortest thermal desorption time (3 s) among the reviewed μ-GC systems.

Micro gas chromatography column (μ-GC column)

The μ-GC column is fabricated by etching a channel with a rectangular cross section and a width and depth in the micrometer scale on the front side of the centimeter-scale silicon and bonding glass on the top side that is open to allow fluids to flow along the channel. In addition, an RTD and a microheater are commonly deposited on the backside for temperature control. Consequently, the walls of the channel are coated with a stationary phase that can interact with VOCs. The separation performance of the μ-GC column can be validated in detail by the following parameters: height equivalent to a theoretical plate (HETP), which refers to the separation efficiency, resolution, selectivity, which refers to the degree of separation

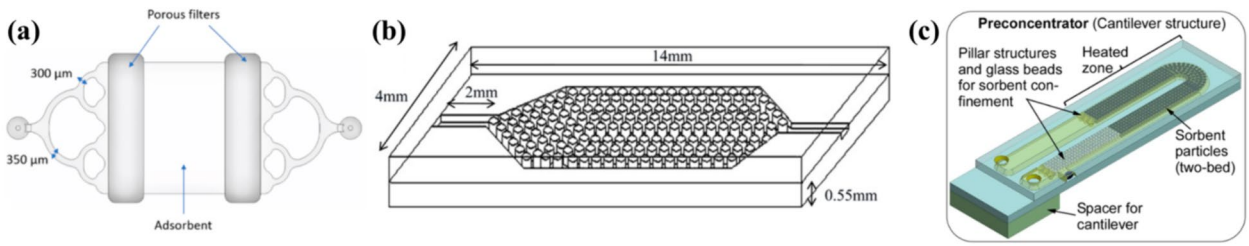

Fig. 7 μ-PCs with enhanced specific characteristics. **a** Manifold-fluidic-system-adopted μ-PC [22] ©2019 MDPI. All rights reserved, **b** microneedle-adopted μ-PC [50] ©2012 Elsevier. All rights reserved, and **c** cantilever-structure-adopted μ-PC [16] ©2016 Springer Nature. All rights reserved

Table 2 Details of PCs and μ-PCs used in the reviewed μ-GC systems

System name	Design	Adsorbent	Preconcentration	Heating method
Zebra GC system [15]	Film on micro post structure	Tenax TA	2 min (1 mL/min)	Cr/Ni patterning (200 °C, 12 s)
iGC3.c2 system [16]	U-shaped-microchannel-embedded cavity	Carbopack B, Carbopack X	10–120 min (0.2 mL/min)	Ti/Pt patterning (250 °C, 15 s)
μGC system [17]	Film on micro post structure	Carbon film	Not described	Ni/Cr wire
2-D GC × GC device [18]	Cavity	Carbopack B	2 min (25 mL/min)	Pt heater (250 °C, 10 s)
PEMM-1 [19]	Cavity	Carbopack B, Carbopack X	1 min (10 mL/min)	Ti/Pt heater (225 °C, 41 s)
PEMM-2 [20]	Cavity	Carbopack B, Carbopack X	1–2 min (5 mL/min)	Ti/Pt heater (225 °C, 41 s)
Compact GC platform [21]	Not described	Carbograph®5, Carbosieve®S-III	10 min	Not described
Compact prototype GC [22]	Cavity	Basolite C300	4 min (5 mL/min)	Heating cartridges (150 °C, 80 s)
Portable GC [23]	Glass tube	CNT sponge	1 min (90 mL/min)	CNT sponge resistance (250 °C, 3 s)
μGC-PID [24]	Stainless-steel tube	Carbopack B, carbopack X	1–10 min (20 mL/min)	Ni/Cr wire

Table 3 Details of GC and μ-GC columns used in the reviewed μ-GC systems

System name	Design	Dimension l (m) × w (μm) × d (μm)	Stationary phase (thickness)	Temperature ramping method	Separation time
Zebra GC system [15]	Not described	2 × 70 × 240	OV-1 (~ 250 nm)	PWM and PID control (35–150 °C)	2 min
iGC3.c2 system[16]	Serpentine type	0.3 m × 230 μm (Hydraulic diameter)	OV-1 (200 nm)	No temperature ramping	10 min
μGC system [17]	Square-spiral type	3 × 100 × 240	OV-1	Feedback loop (ramping to 100 °C)	4 min
2-D GC × GC device [18]	Commercial Rtx-5MS, Rtx-200	10, 3 × 250 (Inner diameter)	5% diphenyl/95% dimethyl PS, PTFPMS (250 nm)	PWM and PID control (50–120 °C)	19 min
PEMM-1 [19]	Square-spiral type	3.1 × 150 × 240	OV-1 (200 nm)	PID control (50–150 °C)	4 min
PEMM-2 [20]	Square-spiral type	2 × 140 × 250	OV-1 (200 nm)	Not described (30–180 °C)	2.5 min
Compact GC platform [21]	Square-spiral type	0.5 × 800 × 700	Carbograph®1, Carbograph®2, Carbograph®5	Not described (30–180 °C)	3–9 min
Compact prototype GC [22]	Commercial RXi-624Sil	20 m × 180 μm (Inner diameter)	6% cyanopropyl/ 94% phenyl PDMS (1,000 nm)	Not described (Isothermal 70 °C)	15 min
Portable GC [23]	Commercial MXT-1	30 m × 280 μm (Inner diameter)	OV-1 (1,000 nm)	PWM and PID control (70–120 °C)	6–10 min
μGC-PID [24]	Not described	5, 10 × 160 × 160	Not described	PWM control (30–80 °C)	2–10 min

between two adjacent peaks, capacity factor, which refers to the degree to which the compound is retained in the stationary phase, and peak asymmetry, which measures the slope of the peak. The design of the μ-GC column has been more extensively studied compared to that of the μ-PC. Research on the design of μ-GC can be divided into three categories based on how to place channels within a chip, how to form a microstructure within a column, and how to modify the shape of the channel [60]. Most design studies have demonstrated the superiority of

the developed designs using HETP, a performance index that indicates that a smaller value is better for separation efficiency. In this chapter, representative μ-GC related to design studies as well as the μ-GC columns of the reviewed systems mentioned in Table 3 were investigated in detail from the design aspect. In terms of the stationary phase, most μ-GCs have adopted PDMS or PDMS-based polymers. Therefore, the review of the stationary phase in this paper only includes the introduction of conventional PDMS and MOFs, which have the potential to serve as a new stationary phase in the GC field.

μ-GC column design

The research on the design of μ-GC columns was broadly divided into three categories: (1) channel arrangement, (2) microstructure within the channel, (3) channel shape. The work conducted by Radadia et al. is considered to demonstrate the most representative channel arrangement [61]. As shown in Fig. 8a–d, the channel arrangement is divided into three types: serpentine, spiral, and square spiral, and each performance was evaluated using the plate number (reciprocal of HETP), which is referred to as the separation efficiency of the column. As a result of the experiment, the spiral and square spiral types showed similar plate numbers in most flow rate sections, whereas the serpentine type demonstrated better separation performance with a relatively high plate number due to its high dispersion force and thin coating thickness with uniformity. However, even though these results were published in 2012, most μ-GC systems used square spiral-type columns, and only the iGC3.c2 system adopted a serpentine-type column (Fig. 8e) [16]. Next, the column design based on the microstructure within the channel is discussed. In empty pipe flow, the velocity distribution across the cross section is the highest at the center and lowest at the walls. This unbalanced flow rate distribution can reduce separation efficiency. The microstructure formed within the channel evenly

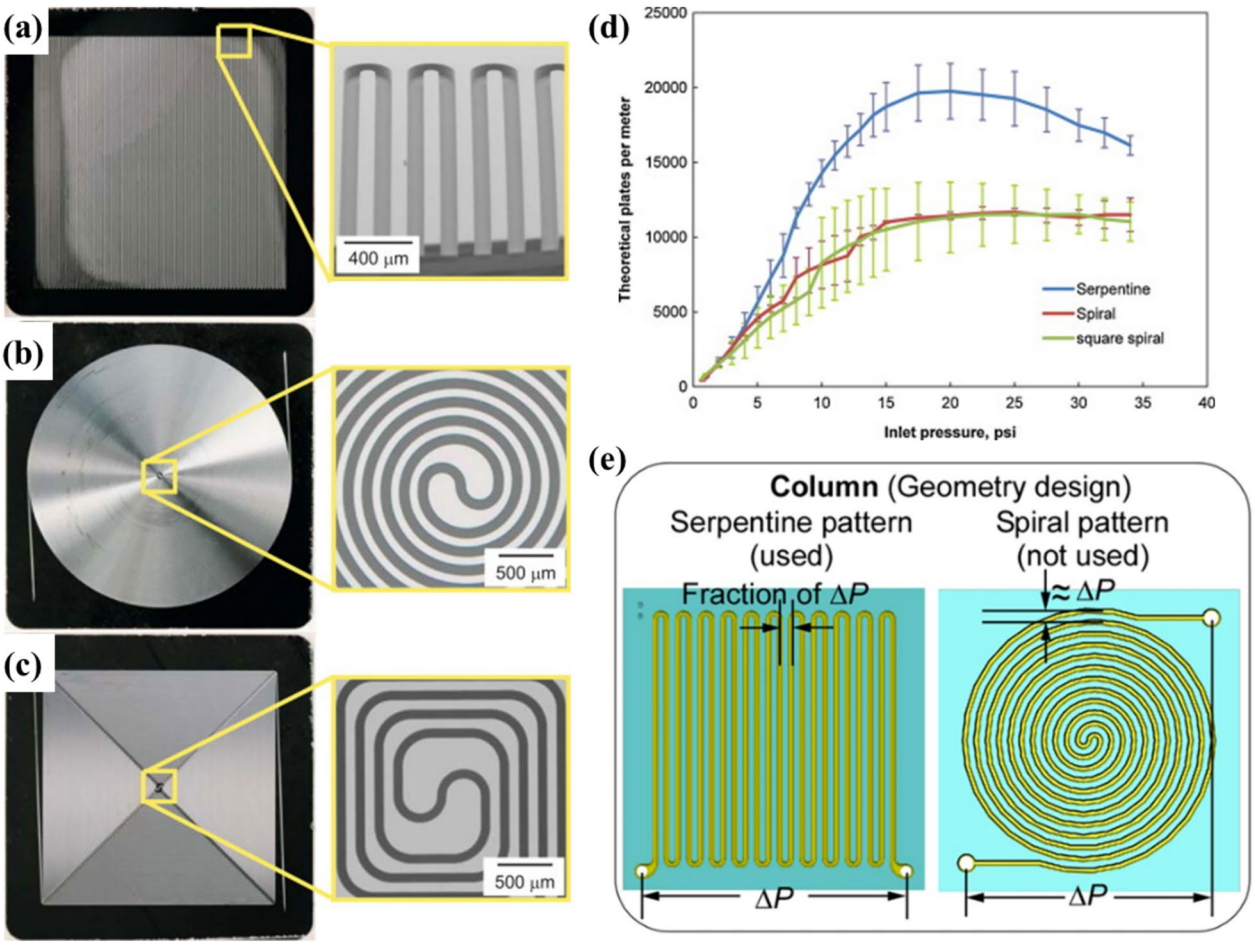

Fig. 8 Channel arrangement of μ-GC columns. **a**–**c** Serpentine, spiral, and square spiral columns, respectively [55] ©2010 Elsevier. All rights reserved, **d** plate numbers for performance testing using the three types of columns [55] ©2010 Elsevier. All rights reserved, and **e** μ-GC column used in the iGC3.c2 system [16] ©2016 Springer Nature. All rights reserved

distributes the flow velocity across the cross section and increases separation efficiency by narrowing the distance between the analyte and the stationary phase, which was first reported in 2009 by Ali et al. [62]. In this study, the microstructures were rectangular, withthree microstructures spaced 30 μm apart within a 150-μm distance (Fig. 9a). Later, Tian et al. and Xue-Lei et al. reported the effects of circular or oval microstructures on separation performance (Fig. 9b,c) [63, 64].

Representative studies on channel shapes can be explained by wavy and bumpy columns. First, the wavy column studied by Yuan et al. in 2017 introduced a structure with alternating up and down arcs of a certain angle, and this angle was optimized for a relatively uniform flow velocity distribution across the column cross section [65]. Ultimately, the performance was verified upon comparison with the HETP obtained using a serpentine column without an arc, as shown in Fig. 9d,e. In 2019, Lee et al. developed a bump column that was geometrically similar to a wavy column but focused on increasing the interaction between the analyte and the stationary phase coated on the wall of the channel. In the bump structure, semicircles are arranged alternately, as shown in Fig. 9f [36]. The bump structure was confirmed to have a higher plate number and separation resolution compared to the other column designs (Fig. 9g). Some μ-GC systems utilize commercial GC instead of μ-GC as it offers reliability and repeatability that can be achieved using long columns and rigid stationary phases. The 2D GC×GC device highlights the 2D GC introduced in the previous chapter using the Rtx-5MS and Rtx-200 columns, as shown in Table 3 [18]. Further, the compact prototype GC emphasizes the performance of the μ-PC based on the symmetric manifold fluidic system using the RXi-624Sil column [22]. In addition, the portable GC highlights the CNT sponge-based μ-PC, developed PID module, and electronic pressure control system using the MXT-1 column [23]. Although commercial GC is appropriate for emphasizing the specific features of the μ-GC system, it inevitably has disadvantages in terms of miniaturization.

μ-GC column stationary phase

Except for commercial columns, PDMS called OV-1 was used as the stationary phase for the μ-GC columns of most μ-GC systems (Table 3). OV-1 is a representative silicon-based nonpolar phase, which is suitable for separating nonpolar and moderately polar VOCs, such as benzene, toluene, ethylbenzene, and xylene [36]. In addition, it is easy to use because it can be inserted into the μ-GC column in liquid form with a crosslinking material and hardened via heating.

Although not used in the reviewed μ-GC systems, MOFs have received immense interest in the past 20 years. MOFs are three-dimensional porous materials composed of bonding between a metal ion and an organic linker and have been studied as an adsorbent or stationary phase because the pore size that accepts VOCs and the functional group that can interact with VOCs

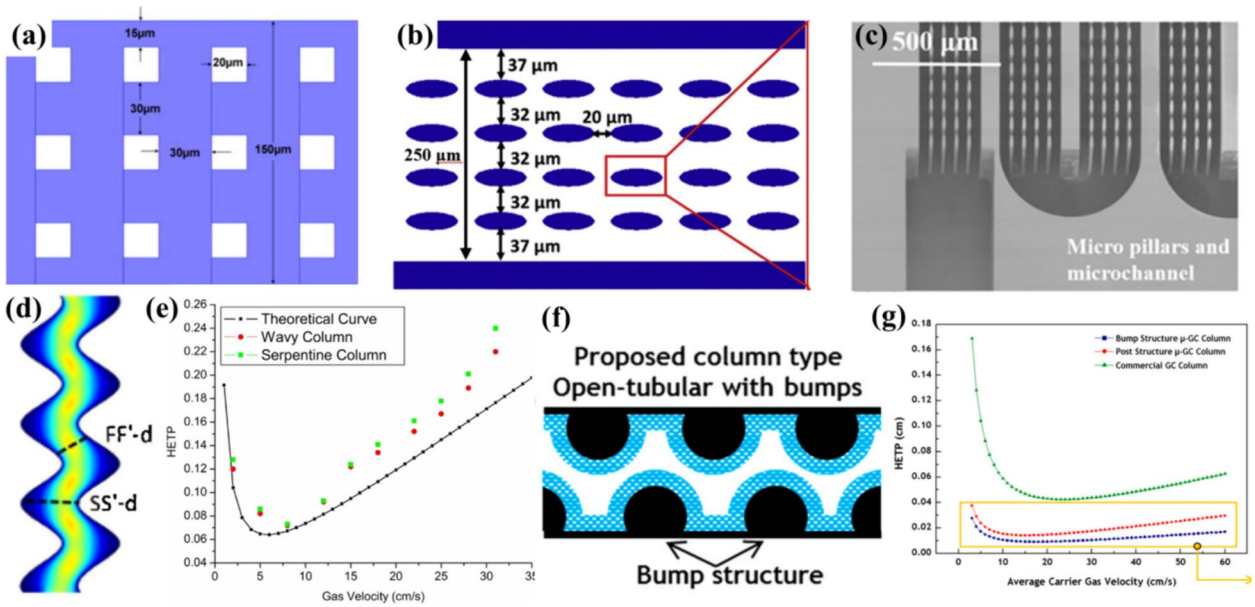

Fig. 9 μ-GC column design based on the microstructure within the channel and channel shape. **a**–**c** Developed microstructure embedded μ-GCs [56] ©2009 Elsevier [57]. ©2018 Elsevier [58]. ©2019 Elsevier. All rights reserved, **d**, **e** wavy μ-GC column and its HETP [59] ©2017 Elsevier. All rights reserved, and **f**, **g** bump μ-GC and HETP [32] ©2019 MDPI. All rights reserved

can be modified freely [66–68]. MOFs with various physical and chemical properties have been applied to commercial fused silica capillary columns and have demonstrated their promise by separating polar and nonpolar VOCs better than conventional stationary phases [69, 70]. The first MOF-coated μ-GC column was developed by Read et al. in 2020 [71]. The HKUST-1/ZIF-8 coated 2D μ-GC column enabled the separation of methane and ethane, which were difficult to separate using a short column owing to weak interaction with the stationary phase and the separation of various harmful VOCs. Tailoring MOF materials and strengthening interaction forces are considered new research topics in short-length μ-GC.

Detectors

As the detectors used in μ-GC systems are utilized in combination with GC, characteristics such as low detection limit, wide quantitative linear range, and fast response and recovery are more important than selectivity. Gas flow rates vary depending on the detector, but they are generally in the range of 1 to 1,000 mL·min^{-1}. This chapter covers the detection mechanisms and configurations of the various detectors applied to μ-GC systems and includes findings obtained using each detector.

Photoionization detector (PID)

The operating principle of the PID is based on the photoionization process, which uses an ultraviolet (UV) lamp to ionize VOC molecules [72]. The PID comprises a UV lamp, ionization chamber, and electrode system, and each device performs UV irradiation and ionization (Fig. 10a). When irradiated with UV light, UV photons collide with VOC molecules, separating electrons from the VOC molecules to form positive ions. The generated ions are collected using electrodes and converted into current signals. The sensitivity of the PID greatly depends on the energy of the UV lamp used, which must exceed the energy required to ionize VOCs, so the lamp must be selected considering the ionization energies of the VOCs to be analyzed. The PID offers excellent response speed, recovery speed, linearity, and sensitivity. The PID-AH2 model from Alphasense, a representative mini-PID

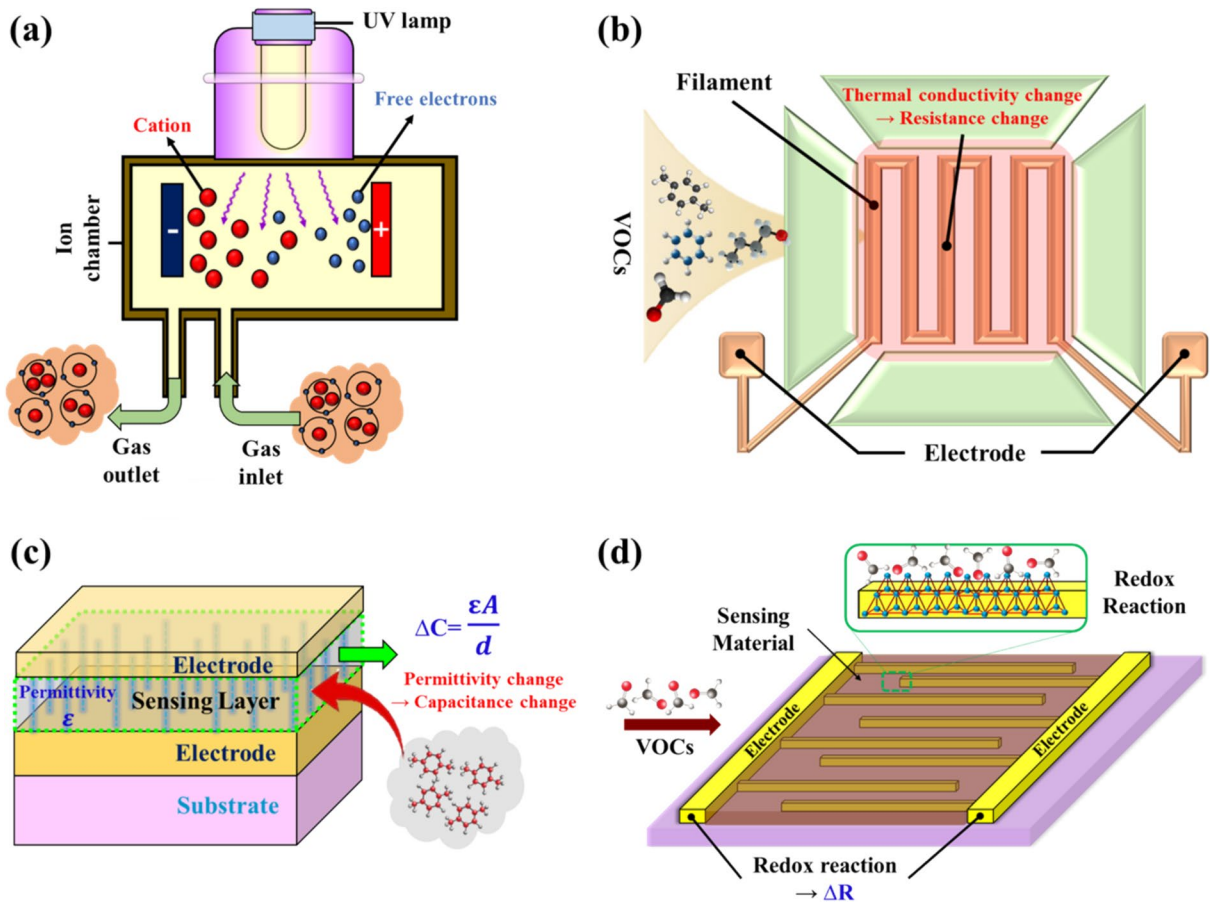

Fig. 10 Configuration diagram including the sensing mechanism of mini/micro-VOC detectors used in μ-GC systems. **a** Photoionization detector (PID), **b** micro-thermal conductivity detector (μ-TCD), **c** capacitive detector, and **d** chemiresistive detector

developer, is known to have a detection limit of 1 ppb for isobutylene, and its size is relatively small, so it can be used in a 2D GC×GC device, portable GC, and compact prototype GC using a commercial GC column [18, 22, 23, 38]. Since 2014, several μ-PIDs have been reported based on MEMS processes applicable to microfluidic systems, and the μGC-PID is considered the first μ-GC system utilizing a μ-PID [24, 72].

Thermal conductivity detector (TCD)

The TCD has a detection mechanism based on the thermal conductivity difference between a carrier gas, such as hydrogen or helium, and targeted VOCs [73, 74]. As shown in Fig. 10b, the TCD comprises a thermally isolated filament, and when VOCs pass through the filament inside the TCD, the resistance of the filament changes owing to the difference in thermal conductivity. Typically, the TCD is placed on each resistor in a Wheatstone bridge circuit. Since the change in resistance due to sensing is not large, the difference in thermal conductivity between the targeted VOCs and the carrier gas must be large. In addition, the filament must be made of a material with high-temperature stability and good thermal conductivity. The Zebra GC system and the compact GC platform applied the TCD to fabricate μ-GC systems [15, 21].

Capacitive detector

Capacitive detectors operate based on the change in permittivity that occurs in the sensing layer as VOCs are injected. Figure 10c shows the structure of the capacitive detector comprising the substrate, electrode, sensing layer, and electrode. The sensing layer generally uses metal oxide or polymer dielectric to provide selectivity for specific VOCs. When a VOC reaches the sensing layer, interactions such as adsorption between the sensing material and the VOC primarily change the permittivity, which secondarily changes the capacitance. This capacitance change is detected as an electrical signal by the electrode. The iGC3.c2 system utilized a capacitive detector featuring two distinct sensing layers, enabling the reconstruction of data from both layers and thereby offering selectivity for gases that cannot be separated using μ-GC [16].

Chemiresistive detector

When the sensing material comes into contact with VOCs, a charge is transferred via the oxidation/reduction or various chemical reactions, causing a change in resistance [75, 76], through which the chemiresistive detector analyzes targeted VOCs. This detector is mainly fabricated by coating with or depositing metal oxides, such as SnO_2 and ZnO, which undergo redox reactions, on interdigitated electrodes. Recently, heterojunctions such as catalysts and filtering layers have been used to maximize detection performance, but metal oxides still present challenges because they require high temperatures for activation, leading to the development of a variety of sensing materials in the form of MOFs or core–shell structures that can be used at room temperature and improve performance [77]. The μGC system, PEMM-1, and PEMM-2 utilized these chemiresistive detectors, and good selectivity was achieved; however, they all utilized arrays with four or five chemiresistor detectors [17, 19, 20].

Challenging issues

Although many commercially available μ-GC systems exist, they are not yet widely distributed [78–80] because the importance of analyzing harmful VOCs in indoor air or biomarker VOCs in human metabolites has not yet been widely recognized, and related legislation or strong sanctions for violations are still lacking. This review excludes these external factors as challenges to the commercialization of μ-GC systems and addresses related technical issues in detail.

The technical challenges of μ-GC systems can be illustrated via application examples. μ-GC systems are useful for analyzing harmful VOCs and warning of hazards in spaces where much time is spent indoors, such as homes and offices. It is especially useful in hospitals, maternity homes, kindergartens, and nursing homes, which can involve many infants, children, and the elderly with medical conditions. In addition, noninvasive disease diagnosis using the analysis of VOC biomarkers in human metabolites is currently a hot research area [81, 82]. Currently, the noninvasive diagnosis of various cancers and Alzheimer's disease using μ-GC systems is being investigated as a simple and inexpensive method for individuals to receive at home or in small clinics [83, 84]. In addition, early diagnosis of various diseases through routine exhaled gas analysis can reduce national healthcare costs and increase life expectancy. To realize these applications, μ-GC systems must be available and deployable in homes, offices, and healthcare facilities. Commercially available μ-GC systems have not been widely adopted owing to their relatively high cost, which is the primary issue that must be resolved for the commercialization and dissemination of μ-GC systems. The high price is largely because mass production facilities have not been established and each of the three essential sections of the platform requires a separate and expensive fabrication process. To address these challenges, the Zebra GC system designs and fabricates μ-GC and μ-TCD in an integrated structure on a single chip to reduce production cost and size [15]. More recently, a MOF-based hybrid

chip that replaces μ-PC and μ-GC with a single device was developed by Lee et al. in 2024 [85]. The development of the main MEMS devices on a single chip and the optimization of the process are essential to reduce the cost of μ-GC systems.

Miniaturization is the second challenge, as it is an important factor in expanding the field of possible applications. Integrating the aforementioned MEMS devices on a single chip can also contribute to miniaturization, but additional steps are needed to achieve ultra-miniaturization. For example, the bidirectional pump of the iGC3.C3 system is particularly suitable for miniaturization because it not only miniaturizes the mini-pump but also eliminates the need for a valve [16]. In addition, the compact GC platform, the smallest platform reported to date, uses a silicon fluidic motherboard to minimize the number of connections between key components, achieving a size of 0.72 L [21]. In addition, owing to the nature of GC, which requires a carrier gas, μ-GC systems involve small cartridges containing high-purity, nonreactive gases, such as helium, hydrogen, and nitrogen. In addition, a pressure regulator is required to allow high-pressure gas to flow through the system at an appropriate flow rate, which in turn affects the size of the μ-GC system. However, in the cases of the μGC system and the compact GC platform, ambient air was used as a carrier gas using a filter pack to filter out dust and organic matter [17, 21], which is also expected to contribute to miniaturization. The consolidation of key components, miniaturization, the elimination of other components (e.g., valves/pumps/carrier gas cartridges), and the minimization of interconnections can contribute significantly to miniaturization, which can broaden the application fields of μ-GC systems.

The third challenge is the reliability of μ-GC systems. Most reported systems present results based on a few experiments in a limited laboratory environment. Among the μ-GC systems reviewed, only the compact prototype GC platform presented the relative standard deviation of the daily analyses conducted for a week [22]. In addition, stability in harsh humidity and temperature conditions must be evaluated.

Finally, there is the issue of selectivity for multispecies VOCs. Hundreds of VOCs exist in indoor air and exhaled breath, and for a μ-GC system to be useful, it must be able to analyze them qualitatively and quantitatively. Often, the lack of selectivity can be overcome using a sensor array, but no portable system with a sensor array has yet been reported to analyze all VOCs in indoor air and exhaled breath. Selectivity is largely a function of the μ-GC system performance and requires novel developments in design and the stationary phase. In this regard, as conventional silicon-based stationary phases have shown limitations in μ-GCs with short channel lengths, MOFs with strong retention force/interaction can be further studied as a new alternative.

Conclusions

The development of μ-GC systems to replace TD–GC–MS has been ongoing for nearly 40 years, starting with a silicon wafer-based μ-GC as one of the core devices. Although the details may vary depending on the researcher's purpose, in general, a μ-GC system is developed using three core components: a μ-PC, a μ-GC column, and a detector. Further, research and development on design and materials are still ongoing to improve preconcentration, separation, and detection. Several commercialized μ-GC systems can serve as air quality analyzers and noninvasive disease diagnostic instruments. However, the supply and broad utilization have remained difficult owing to shortcomings in terms of size and cost. In addition, core devices that can qualitatively and quantitatively analyze all VOCs present in indoor air and exhaled gas must be developed. New materials such as MOFs may improve the performances of μ-GC systems and enable one-chip integration for miniaturization and cost reduction. The development of these materials is the key to overcoming a major hurdle for the commercialization of μ-GC systems.

Abbreviations

VOCs	Volatile organic compounds
μ-GC system	Micro-gas chromatography system
TD–GC–MS	Thermal desorption–gas chromatography–mass spectrometry
μ-PC	Micro-gas preconcentrator
TD	Thermal desorption
PDMS	Polydimethylsiloxane
DRIE	Deep reactive ion etching
RTD	Resistive temperature detector
RT	Retention time
PID	Photoionization detector
FID	Flame ionization detector
μ-TCD	Micro-thermal conductivity detector
FMB	Silicon fluidic motherboard
MOF	Metal–organic framework
HETP	Height equivalent to a theoretical plate
UV	Ultraviolet

Author contributions

YL conducted the literature survey and prepared the first draft. HS and JL helped in writing the manuscript and drawing the schematics. SHL acquired the financial support and reviewed and edited the manuscript. All authors read and approved the final manuscript.

Funding

This study was supported by the National Research Foundation, funded by the Ministry of Science and ICT [grant number: 2020R1A2C2101798] and the Ministry of the Interior and Safety R&D program [grant number: 20018500], Republic of Korea.

Availability of data and materials

The data and materials are available from the corresponding author on reasonable request.

Declarations

Competing interests

The authors declare that they have no competing interests.

Received: 18 April 2024 Accepted: 5 June 2024
Published online: 13 June 2024

References

1. Nakaoka H, Todaka E, Seto H, Saito I, Hanazato M, Watanabe M, Mori C (2014) Correlating the symptoms of sick-building syndrome to indoor VOCs concentration levels and odour. Indoor Built Environ 23:804–813. https://doi.org/10.1177/1420326X13500975
2. Sun Y, Hou J, Cheng R, Sheng Y, Zhang X, Sundell J (2019) Indoor air quality, ventilation and their associations with sick building syndrome in Chinese homes. Energy Build 197:112–119. https://doi.org/10.1016/j.enbuild.2019.05.046
3. Xu Y, Zhang Y (2003) An improved mass transfer based model for analyzing VOC emissions from building materials. Atmos Environ 37:2497–2505. https://doi.org/10.1016/S1352-2310(03)00160-2
4. Liu Z, Ye W, Little JC (2013) Predicting emissions of volatile and semivolatile organic compounds from building materials: a review. Build Environ 64:7–25. https://doi.org/10.1016/j.buildenv.2013.02.012
5. Boor BE, Järnström H, Novoselac A, Xu Y (2014) Infant exposure to emissions of volatile organic compounds from crib mattresses. Environ Sci Technol 48:3541–3549. https://doi.org/10.1021/es405625q
6. Maung TZ, Bishop JE, Holt E, Turner AM, Pfrang C (2022) Indoor air pollution and the health of vulnerable groups: a systematic review focused on particulate matter (PM), volatile organic compounds (VOCs) and their effects on children and people with pre-existing lung disease. Int J Environ Res Public Health. https://doi.org/10.3390/ijerph19148752
7. IARC (2021) Agents classified by the IARC monographs for cancer on WHO report. IARC. 2021:1–37. https://monographs.iarc.who.int/agents-classified-by-the-iarc. Accessed 16 Apr 2024.
8. Pathak AK, Swargiary K, Kongsawang N, Jitpratak P, Ajchareeyasoontorn N, Udomkittivorakul J, Viphavakit C (2023) Recent advances in sensing materials targeting clinical volatile organic compound (VOC) biomarkers: a review. Biosensors (Basel). https://doi.org/10.3390/bios13010114
9. Saalberg Y, Wolff M (2016) VOC breath biomarkers in lung cancer. Clin Chim Acta 459:5–9. https://doi.org/10.1016/j.cca.2016.05.013
10. Gallego E, Roca FJ, Perales JF, Sánchez G, Esplugas P (2012) Characterization and determination of the odorous charge in the indoor air of a waste treatment facility through the evaluation of volatile organic compounds (VOCs) using TD-GC/MS. Waste Manag 32:2469–2481. https://doi.org/10.1016/j.wasman.2012.07.010
11. Kaikiti C, Stylianou M, Agapiou A (2022) TD-GC/MS analysis of indoor air pollutants (VOCs, PM) in hair salons. Chemosphere 294:133691. https://doi.org/10.1016/j.chemosphere.2022.133691
12. Son B, Breysse P, Yang W (2003) Volatile organic compounds concentrations in residential indoor and outdoor and its personal exposure in Korea. Environ Int 29:79–85. https://doi.org/10.1016/S0160-4120(02)00148-4
13. USEP Agency (2017) Method 8260D: volatile organic compounds by gas chromatography/mass spectrometry. SW-864 Update VI. https://www.epa.gov/sites/default/files/2017-04/documents/method_8260d_update_vi_final_03-13-2017.pdf. Accessed 16 Apr 2024.
14. Collin WR, Serrano G, Wright LK, Chang H, Nuñovero N, Zellers ET (2014) Microfabricated gas chromatograph for rapid, trace-level determinations of gas-phase explosive marker compounds. Anal Chem 86:655–663. https://doi.org/10.1021/ac402961t
15. Garg A, Akbar M, Vejerano E, Narayanan S, Nazhandali L, Marr LC, Agah M (2015) A mini gas chromatography system for trace-level determination of hazardous air pollutants. Sens Actuators B 212:145–154. https://doi.org/10.1016/j.snb.2014.12.136
16. Qin Y, Gianchandani YB (2016) A fully electronic microfabricated gas chromatograph with complementary capacitive detectors for indoor pollutants. Microsyst Nanoeng 2:15049. https://doi.org/10.1038/micronano.2015.49
17. A portable micro gas chromatography system for lung cancer associated volatile organic compound detection (2016). IEEE J Solid State Circuits 51:259–272. https://doi.org/10.1109/JSSC.2015.2489839.
18. Lee J, Zhou M, Zhu H, Nidetz R, Kurabayashi K, Fan X (2016) Fully automated portable comprehensive 2-dimensional gas chromatography device. Anal Chem 88:10266–10274. https://doi.org/10.1021/acs.analchem.6b03000
19. Wang J, Bryant-Genevier J, Nuñovero N, Zhang C, Kraay B, Zhan C, Scholten K, Nidetz R, Buggaveeti S, Zellers ET (2018) Compact prototype microfabricated gas chromatographic analyzer for autonomous determinations of VOC mixtures at typical workplace concentrations. Microsyst Nanoeng. https://doi.org/10.1038/micronano.2017.101
20. Wang J, Nuñovero N, Nidetz R, Peterson SJ, Brookover BM, Steinecker WH, Zellers ET (2019) Belt-mounted micro-gas-chromatograph prototype for determining personal exposures to volatile-organic-compound mixture components. Anal Chem 91:4747–4754. https://doi.org/10.1021/acs.analchem.9b00263
21. Zampolli S, Elmi I, Cardinali GC, Masini L, Bonafè F, Zardi F (2020) Compact-GC platform: a flexible system integration strategy for a completely microsystems-based gas-chromatograph. Sens Actuators B. https://doi.org/10.1016/j.snb.2019.127444
22. Lara-Lbeas I, Rodríguez-Cuevas A, Andrikopoulou C, Person V, Baldas L, Colin S, Le Calvé S (2019) Sub-ppb level detection of BTEX gaseous mixtures with a compact prototype GC equipped with a preconcentration unit. Micromachines (Basel). https://doi.org/10.3390/mi10030187
23. You DW, Seon YS, Jang Y, Bang J, Oh JS, Jung KW (2020) A portable gas chromatograph for real-time monitoring of aromatic volatile organic compounds in air samples. J Chromatogr A 1625:461267. https://doi.org/10.1016/j.chroma.2020.461267
24. Wei-Hao Li M, Ghosh A, Venkatasubramanian A, Sharma R, Huang X, Fan X (2021) High-sensitivity micro-gas chromatograph-photoionization detector for trace vapor detection. ACS Sens 6:2348–2355. https://doi.org/10.1021/acssensors.1c00482
25. Lu CJ, Steinecker WH, Tian WC, Oborny MC, Nichols JM, Agah M et al (2005) First-generation hybrid MEMS gas chromatograph. Lab Chip 5(10):1123–1131. https://doi.org/10.1039/b508596a
26. Lussac E, Barattin R, Cardinael P, Agasse V (2016) Review on micro-gas analyzer systems: feasibility, separations and applications. Crit Rev Anal Chem 46(6):455–468. https://doi.org/10.1080/10408347.2016.1150153
27. Regmi BP, Agah M (2018) Micro gas chromatography: an overview of critical components and their integration. Anal Chem 90(22):13133–13150. https://doi.org/10.1021/acs.analchem.8b01461
28. Haghighi F, Talebpour Z, Sanati-Nezhad A (2015) Through the years with on-a-chip gas chromatography: a review. Lab Chip 15(12):2559–2575. https://doi.org/10.1039/c5lc00283d
29. UNITY Document (n.d.) XR. https://docs.unity3d.com/Manual/XR.html. Accessed 16 Apr 2024.
30. Agilent (n.d.) 5977C GC/MSD. GC/MS Instruments. https://www.agilent.com/en/product/gas-chromatography-mass-spectrometry-gc-ms/gc-ms-instruments/5977c-gc-msd. Accessed 16 Apr 2024.
31. MARKES International (n.d.) Sorbent tubes - glass. https://markes.com/samplingtechnologies/supplies-collection/sorbent-tubes-glass. Accessed 16 Apr 2024.
32. Lee J, Lee J, Lim SH (2020) Micro gas preconcentrator using metal organic framework embedded metal foam for detection of low-concentration volatile organic compounds. J Hazard Mater 392:122145. https://doi.org/10.1016/j.jhazmat.2020.122145
33. YMC (n.d.) Packed column. https://ymc.sg/products/ymc-pack-c8/. Accessed 16 Apr 2024.
34. RESTEK (n.d.) Capillary column. https://www.restek.com/global/en/p/11140. Accessed 16 Apr 2024.
35. Agilent Technologies (2012) Agilent 5975 Series MSD: Operation Manual. https://www.agilent.com/cs/library/usermanuals/public/G3170-90036.pdf. Accessed 16 Apr 2024.
36. Lee J, Lim SH (2019) Development of Open-tubular-type micro gas chromatography column with bump structures. Sensors (Basel). https://doi.org/10.3390/s19173706
37. ThermoFisher Scientific (n.d.) iConnect™ flame ionization detector (FID) for TRACE™ 1300 and 1600 series GC. https://www.thermofisher.com/

order/catalog/product/19070001?SID=srch-hj-19070001. Accessed 16 Apr 2024.
38. Alphasense AMETEK (n.d.) PID-AH2 photo ionisation detector. https://ametekcdn.azureedge.net/mediafiles/project/oneweb/oneweb/alphasense/products/datasheets/alphasense_pid-ah2_datasheet_en_1.pdf?revision:bf5b3e8a-c6a3-4608-ae2e-b3b91032485b. Accessed 16 Apr 2024.
39. FIERCE Electronics (2018) Metal oxide gas sensing material and MEMS process. https://www.fierceelectronics.com/components/metal-oxide-gas-sensing-material-and-mems-process. Accessed 16 Apr 2024.
40. Ho CK, Hughes RC (2002) In-situ chemiresistor sensor package for real-time detection of volatile organic compounds in soil and groundwater. Sensors 2:23–34. https://doi.org/10.3390/s20100023
41. Dave SB (1969) A comparison of the chromatographic properties of porous polymers. J Chrmatographic Sci 7:389–399. https://doi.org/10.1093/chromsci/7.7.389
42. Terry SC, Jerman JH, Angell JB (1979) A gas chromatographic air analyzer fabricated on a silicon wafer. IEEE Trans Electron Devices 26:1880–1886. https://doi.org/10.1109/T-ED.1979.19791
43. McCartney MM, Zrodnikov Y, Fung AG, LeVasseur MK, Pedersen JM, Zamuruyev KO, Aksenov AA, Kenyon NJ, Davis CE (2017) An easy to manufacture micro gas preconcentrator for chemical sensing applications. ACS Sens 2:1167–1174. https://doi.org/10.1021/acssensors.7b00289
44. Bryant-Genevier J, Zellers ET (2015) Toward a microfabricated preconcentrator-focuser for a wearable micro-scale gas chromatograph. J Chromatogr A 1422:299–309. https://doi.org/10.1016/j.chroma.2015.10.045
45. Stolarczyk A, Jarosz T (2022) Micropreconcentrators: recent progress in designs and applications. Sensors (Basel). https://doi.org/10.3390/s22041327
46. Lahlou H, Vilanova X, Correig X (2013) Gas phase micro-preconcentrators for benzene monitoring: a review. Sens Actuators, B Chem 176:198–210. https://doi.org/10.1016/j.snb.2012.10.004
47. Wang Y, Chen Z, Chen Q, Tian E, Han N, Mo J (2024) Preconcentrating sensor systems toward indoor low-concentration VOC detection by goal-oriented, sequential, inverse design strategy. Build Environ 254:111372. https://doi.org/10.1016/j.buildenv.2024.111372
48. Lara-Ibeas I, Rodríguez Cuevas A, Le Calvé S. Recent developments and trends in miniaturized gas preconcentrators for portable gas chromatography systems: a review. Sensors Actuators B Chem. 346:130449. https://doi.org/10.1016/j.snb.2021.130449.
49. Serrano G, Sukaew T, Zellers ET (2013) Hybrid preconcentrator/focuser module for determinations of explosive marker compounds with a micro-scale gas chromatograph. J Chromatogr A 1279:76–85. https://doi.org/10.1016/j.chroma.2013.01.009
50. Woellner M, Hausdorf S, Klein N, Mueller P, Smith MW, Kaskel S (2018) Adsorption and detection of hazardous trace gases by metal-organic frameworks. Adv Mater 30:e1704679. https://doi.org/10.1002/adma.201704679
51. Goldoust R, Rahbarpour S (2018) Design and implementation of a preconcentrator with zeolite NaY for sensitivity enhancement of commercial gas sensors at low NO2 concentrations. Mater Res Express. https://doi.org/10.1088/2053-1591/aae3a4
52. Ueno Y, Horiuchi T, Morimoto T, Niwa O (2001) Microfluidic device for airborne BTEX detection. Anal Chem 73:4688–4693. https://doi.org/10.1021/ac010210+
53. Pijolat C, Camara M, Courbat J, Viricelle J, Briand D, Derooij N (2007) Application of carbon nano-powders for a gas micro-preconcentrator. Sens Actuators B 127:179–185. https://doi.org/10.1016/j.snb.2007.07.029
54. Alfeeli B, Cho D, Ashraf-Khorassani M, Taylor LT, Agah M (2008) MEMS-based multi-inlet/outlet preconcentrator coated by inkjet printing of polymer adsorbents. Sens Actuators B 133:24–32. https://doi.org/10.1016/j.snb.2008.01.063
55. Halder S, Xie Z, Nantz MH, Fu XA (2022) Integration of a microprecentrator with solid-phase microextraction for analysis of trace volatile organic compounds by gas chromatography-mass spectrometry. J Chromatogr A 1673:463083. https://doi.org/10.1016/j.chroma.2022.463083
56. Wong MY, Cheng WR, Liu MH, Tian WC, Lu CJ (2012) A preconcentrator chip employing mu-SPME array coated with in-situ-synthesized carbon adsorbent film for VOCs analysis. Talanta 101:307–313. https://doi.org/10.1016/j.talanta.2012.09.031
57. Ruiz AM, Gràcia I, Sabaté N, Ivanov P, Sánchez A, Duch M, Gerbolés M, Moreno A, Cané C (2007) Membrane-suspended microgrid as a gas preconcentrator for chromatographic applications. Sens Actuators A 135:192–196. https://doi.org/10.1016/j.sna.2006.07.005
58. Chowdhury AR, Lee T, Day C, Hutter T (2022) A review of preconcentrator materials, flow regimes and detection technologies for gas adsorption and sensing. Adv Mater Interfaces. https://doi.org/10.1002/admi.202200632
59. Alfeeli B, Jain V, Johnson RK, Beyer FL, Heflin JR, Agah M (2011) Characterization of poly(2,6-diphenyl-*p*-phenylene oxide) films as adsorbent for microfabricated preconcentrators. Microchem J 98:240–245. https://doi.org/10.1016/j.microc.2011.02.006
60. Azzouz I, Marty F, Bourouina T (2017) Recent Advances in Micro-Gas chromatography - the opportunities and the challenges. In: Design, test, integration and packaging of MEMS/MOEMS. https://doi.org/10.1109/DTIP.2017.7984485.
61. Radadia AD, Salehi-Khojin A, Masel RI, Shannon MA (2010) The effect of microcolumn geometry on the performance of micro-gas chromatography columns for chip scale gas analyzers. Sens Actuators B 150:456–464. https://doi.org/10.1016/j.snb.2010.07.002
62. Ali S, Ashraf-Khorassani M, Taylor LT, Agah M (2009) MEMS-based semi-packed gas chromatography columns. Sens Actuators B 141:309–315. https://doi.org/10.1016/j.snb.2009.06.022
63. Tian B, Zhao B, Feng F, Luo F, Zhou H, Ge X, Yanhong W, Li X (2018) A micro gas chromatographic column with embedded elliptic cylindrical posts. J Chromatogr A 1565:130–137. https://doi.org/10.1016/j.chroma.2018.06.036
64. Yang X-L, Zhao B, Feng F, Zhou H, Yang H, Li X (2019) High performance micro gas chromatography column using mesoporous silica as stationary phase. Chin J Anal Chem 47:832–837. https://doi.org/10.1016/S1872-2040(19)61164-3
65. Yuan H, Du X, Tai H, Li Y, Zhao X, Guo P, Yang X, Su Y, Xiong Z, Xu M (2017) The effect of the channel curve on the performance of micromachined gas chromatography column. Sens Actuators B 239:304–310. https://doi.org/10.1016/j.snb.2016.08.003
66. Wu H, Gong Q, Olson DH, Li J (2012) Commensurate adsorption of hydrocarbons and alcohols in microporous metal organic frameworks. Chem Rev 112:836–868. https://doi.org/10.1021/cr200216x
67. Ali Akbar Razavi S, Morsali A (2019) Linker functionalized metal-organic frameworks. Coord Chem Rev. https://doi.org/10.1016/j.ccr.2019.213023
68. Li JR, Sculley J, Zhou HC (2012) Metal-organic frameworks for separations. Chem Rev 112:869–932. https://doi.org/10.1021/cr200190s
69. Gu ZY, Jiang JQ, Yan XP (2011) Fabrication of isoreticular metal-organic framework coated capillary columns for high-resolution gas chromatographic separation of persistent organic pollutants. Anal Chem 83:5093–5100. https://doi.org/10.1021/ac200646w
70. Meng SS, Tao ZR, Tang WQ, Han T, Du Y, Gu ZY (2020) Ultramicroporous metal-organic frameworks for capillary gas chromatographic separation. J Chromatogr A 1632:461604. https://doi.org/10.1016/j.chroma.2020.461604
71. Read DH, Sillerud CH, Whiting JJ, Achyuthan KE (2020) Metal-organic framework stationary phases for one- and two-dimensional micro-gas chromatographic separations of light alkanes and polar toxic industrial chemicals. J Chromatogr Sci 58:389–400. https://doi.org/10.1093/chromsci/bmaa005
72. Coelho Rezende G, Le Calvé S, Brandner JJ, Newport D (2019) Micro photoionization detectors. Sens Actuators B 287:86–94. https://doi.org/10.1016/j.snb.2019.01.072
73. Sun JH, Cui DF, Chen X, Zhang LL, Cai HY, Li H (2013) A micro gas chromatography column with a micro thermal conductivity detector for volatile organic compound analysis. Rev Sci Instrum 84:025001. https://doi.org/10.1063/1.4789526
74. Cruz D, Chang J, Showalter S, Gelbard F, Manginell R, Blain M (2007) Microfabricated thermal conductivity detector for the micro-ChemLab™. Sens Actuators B 121:414–422. https://doi.org/10.1016/j.snb.2006.04.107
75. Baharuddin AA, Ang BC, Haseeb ASMA, Wong YC, Wong YH (2019) Advances in chemiresistive sensors for acetone gas detection. Mater Sci Semicond Process. https://doi.org/10.1016/j.mssp.2019.104616
76. Franco MA, Conti PP, Andre RS, Correa DS (2022) A review on chemiresistive ZnO gas sensors. Sens Actuators Rep. https://doi.org/10.1016/j.snr.2022.100100

77. Jo YM, Jo YK, Lee JH, Jang HW, Hwang IS, Yoo DJ (2023) MOF-based chemiresistive gas sensors: toward new functionalities. Adv Mater 35:e2206842. https://doi.org/10.1002/adma.202206842
78. Defiant Technologies (n.d.) FROG-5000™ portable GC PID, micro gas chromatograph with photoionization detector volatile organic compound (VOC) analysis for air, water, and soil samples. https://www.defiant-tech.com/frog-portable-gas-chromatograph-gc/. Accessed 16 Apr 2024.
79. Defiant Technologies (n.d.) VOCAM™ (volatile organic chemical air monitor) portable GC PID, gas chromatograph with photoionization detector for detecting volatile organic compound (VOCs) in air. https://www.defiant-tech.com/vocam-portable-gas-chromatograph-gc/. Accessed on 16 Apr 2024.
80. Dräger (n.d.) Dräger X-pid® 9000/9500. https://www.draeger.com/en_in/Products/X-pid-9000-9500. Accessed 16 Apr 2024.
81. Wu X, Wang D, Shi L, Wang H, Wang J, Sun J, Li C, Tian X (2022) A compact gas chromatography platform for detection of multicomponent volatile organic compounds biomarkers. Rev Sci Instrum 93:065003. https://doi.org/10.1063/5.0086618
82. Wu L, Qu X (2015) Cancer biomarker detection: recent achievements and challenges. Chem Soc Rev 44:2963–2997. https://doi.org/10.1039/c4cs00370e
83. Gregis G, Sanchez J, Bezverkhyy I, Guy W, Berger F, Fierro V, Bellat J, Celzard A (2018) Detection and quantification of lung cancer biomarkers by a micro-analytical device using a single metal oxide-based gas sensor. Sens Actuators B 255:391–400. https://doi.org/10.1016/j.snb.2017.08.056
84. Paraskevaidi M, Allsop D, Karim S, Martin FL, Crean S (2020) Diagnostic biomarkers for Alzheimer's disease using non-invasive specimens. J Clin Med. https://doi.org/10.3390/jcm9061673
85. Lee Y, Choi Y, Sim J, Kim J, Lim SH (2024) Metal-organic framework-based high-performance column chip for micro gas chromatography: hybrid function for simultaneous preconcentration and separation of volatile organic compounds. Lab Chip 24:658–667. https://doi.org/10.1039/d3lc00777d

Publisher's Note

Yeongseok Lee is a doctoral student in the Department of Mechanical Systems at Kookmin University, Republic of Korea. He is currently working on the development of MEMS-based preconcentration, separation, and detection devices for analyzing multiple chemical compounds in the fields of health, safety, and the environment.

Hyunwoo Son is a master's student in the Department of Mechanical Systems at Kookmin University, Republic of Korea. His research interests include the development of MEMS-based detectors.

Junwoo Lee is an undergraduate student in the School of Mechanical Engineering at Kookmin University, Republic of Korea. His research field is the miniaturization of μ-GC systems by one-chip integration.

Si-Hyung Lim received his B.S. and M.S. degrees in Mechanical Design and Production Engineering from Seoul National University, Republic of Korea, in 1994 and 1996, respectively, and his Ph.D. degree in Mechanical Engineering from the University of California, Berkeley, USA, in 2005. He worked as a postdoctoral researcher at the Center of Integrated Nanomechanical Systems and Berkeley Nanoscience and Nanoengineering Institute, the University of California, Berkeley, USA, from 2005 to 2007. He is currently a professor and the supervisor of the Nanomechatronics Laboratory in the School of Mechanical Engineering, Kookmin University, Republic of Korea. His present research focuses on integrated micro-gas analysis systems for environmental and medical applications.